The Topology of Three-dimensional Flows about Blunt Bodies for Low Values of the Reynolds Number.

Marcos A. Ortega, ortega@ita.br
Roberto M. Girardi, girardi@ita.br
ITA - Technological Institute of Aeronautics, São José dos Campos, SP, Brazil

Jorge H. Silvestrini, jorgehs@pucrs.br
PUC/RS - Pontifical Catholic University, Porto Alegre, RS, Brazil

Abstract. *It is well known today that, for three-dimensional flows about two-dimensional geometries, the distribution of Strouhal number as function of the Reynolds number, for low values of the latter parameter, is not smooth. The discontinuities are due to the so called streamwise instabilities which ultimately generate elongated structures developing at the braids of the crosswise basic formations. The main aim of this work is to start an investigation of these phenomena in the case of a blunt-trailing-edged body of various aspect ratios and compare results with the case of the circular cylinder. The investigation tool is a DNS numerical code.*

Keywords: *Blunt body; Three-dimensional flow; Numerical Simulation*

1. INTRODUCTION

There have been, during the eighties of the last century, a renewed interest upon investigations related to blunt bodies. The main aim of those works was evidently the straight cylinder with a circular cross section. Both experimental and numerical strategies were employed. With the advent of massive computation direct numerical simulations were properly fit for the investigation at the lower range of the Reynolds number. Probably the problem that attracted the most of attention was the discontinuities at the Strouhal-Reynolds dependency.

The first indications and measurements related to those discontinuities in the case of the circular cylinder appeared in the works of Roshko (1954) and Tritton (1959), still in the fifties of the twentieth century. As indicated by Williamson (1996) there are three discontinuities in the line representing the relationship between the Strouhal number, representing the fundamental frequency of the wake, and the Reynolds number, characterizing the actual type of flow, in the low range of this parameter up to 300 (not taken into account, evidently, the first bifurcation corresponding to the beginning of vortex shedding). The first one (apparently, the one first observed by Tritton, 1959), that can as well be called a pseudo-discontinuity, is completely inside the laminar region and appears at about $Re = 64$. What happens here is a transition between two states of oblique shedding (Williamson, 1989). The second break in the line ensues at about $Re \simeq 180 - 190$ and the third around 250 (see Fig. 1). In fact the two breaks are the result of the same physical manifestation. The first is mostly known in the literature as "mode A" and the second as "mode B". Roshko (1954) was the first to comment about this phenomenon, calling attention to the scattering of measured data between Reynolds numbers 160 and 300. As the number of Reynolds grows, modes A and B together, and in this order, provides for the transition from a laminar to a turbulent wake .

End effects, that is, the conditions at which the cylinder is fixed at the wall of the wind tunnel, might have an influence upon the appearance of modes A and B. This probably explains the scattering in the literature of the Reynolds number values corresponding to the appearance of those discontinuities. But, there is no doubt today that this is an intrinsic feature of the three-dimensional shedding characteristic of bluff bodies. A Floquet stability analysis of this problem by Barkley and Henderson (1995) arrived at $Re = 188.5 \pm 1.0$ for the critical Reynolds number of mode A. In reality, the main differences between modes A and B are related to the characteristic dimensions and the original instabilities of the streamwise vorticity structures that appear in the flow. At the discontinuity interval what happens is an energy swapping between the two modes with the prevalence of mode B as the Reynolds number grows (Williamson, 1988). At the end of transition one has, what one would recognize by standard criteria, a turbulent flow.

Another point that deserves to be noticed is related to the seeds of instabilities. That is, what kind of de-stabilizing mechanism has to be present for the establishing of modes A and B. This point was the reason for considerable debate in the literature — see, for example, the works of Henderson (1997) and Thompson, Leweke and Williamson (2001). Anyway, there is at least no quarelling about the facts that mode A corresponds to an instability in the core of the primary vortical structures — the laminar Kármán vortices that are shed, and that mode B is mostly related to fluctuations of the primary shear layers (Braza, Chassaing and Ha Minh, 1990, Williamson, 1996).

The objective of this paper is a study of three-dimensional flows of two basic geometrical forms. The first is the circular cross-sectional cylinder and the second is the one we shall call "body of Bearman" — a two-dimensional form whose frontal part is formed by an elliptical nose followed by two parallel plates which end at a blunt base (Bearman, 1965). In principle, three-dimensional forms are obtained by considering that each of these geometries receives an infinite
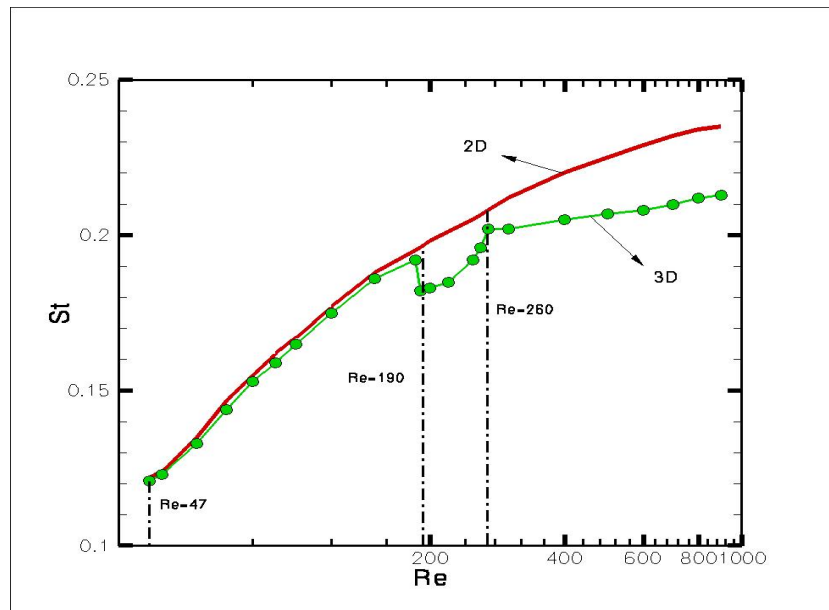
Figure 1. Functional dependence of shedding frequency, represented by the number of Strouhal, St, upon the Reynolds number, Re. Solid line is a curve fit to two-dimensional simulation data; Symbols: experimental data due to Williamson (1989). (Adapted from figure 3 of Henderson, 1997.)

length along the spanwise direction. The analyses will be based on a DNS ("Direct Numerical Simulation") numerical code. Initial results and related discussions of both geometrical forms will be presented.

2. NUMERICAL STRATEGY

The numerical code, named Incompact3d, a multi-purpose code for incompressible flows, was developed in its basic configuration by Lamballais and Silvestrini (2002). Some subroutines were aggregated by the present authors in order to develop the sufficient capability for investigating in detail the associated periodical flow (the coherent structures) and the calculation of forces that actuate upon a body which is immersed in the flow. The main characteristics of Incompact3d are listed below.

- Solves the two- and three-dimensional incompressible Navier-Stokes equations, and uses a 'pressure-based type' strategy, what means that a Poisson equation is associated to the calculation. Besides, an advection-diffusion equation for a passive scalar is also aggregated to the modelling.

- Strategies of solution: DNS and LES.

- Advancement in time. Realized by means of a third-order low-storage Runge-Kutta strategy. Part of the forcing terms in the immersed boundary sub-routine are advanced implicitly, instead, and the Crank-Nicolson scheme is used. This feature improves the efficiency of the forcing mechanism (Fadlun 2000; Lamballais & Silvestrini 2002).

- Space discretization. Spatial derivatives are approximated by a sixth-order compact finite-difference scheme (Lele 1992), except near the inflow and outflow boundaries where single-sided schemes are employed for the x-derivative calculation.

- Poisson equation. If the longitudinal flow direction — the main direction of flow — is periodic the equation is completely resolved in spectral space, otherwise, a mixed method is applied where part of the equation is discretized in physical space and part in spectral space (Lamballais 1996).

- Boundary conditions at solid surfaces. Simulated by virtue of the so called 'immersed boundary' technique. An externally imposed body force, that may vary in space and time, is established along pre-defined surfaces, whose magnitude and direction is such as to oppose the local flow (Goldstein, Handler & Sirovich 1993). Enforcing no-slip boundary conditions in such way permits the discretization on an uniform Cartesian grid, an outstanding advantage.

Code Incompact3d has been already tested in a variety of applications to flows of interest, both two- and three-dimensional. (For specific numerical details, including code validation and verification, the interested reader is referred to the cited papers and works.) Lamballais & Silvestrini (2002) and Silvestrini & Lamballais (2004) have performed very

complex simulations of the wake flow behind a circular cylinder, including the study of the interference of a mixing layer with the wake, and a case of oblique shedding. In the latter situation the stream approaching the cylinder is considered to have a linear shear distribution, what does not allow the system to be considered of infinite spanwise extent. The code has performed very well and results are really promising. (See also Lardeau, Lamballais & Bonnet 2002.) In another type of application the two-dimensional flow about a NACA-0012 profile was simulated up to an angle of attack of thirty degrees (Ortega & Silvestrini 2004). The Reynolds number of the simulations was equal to 1000, based on the foil chord. In this instance, the present authors aggregated to Incompact3d a certain number of sub-routines which brought to the code the capability of calculating forces (using the control volume technique). (See also Ortega, Girardi & Silvestrini 2007.) A very important overall analysis was carried out by Ribeiro (2002). The code works in practice as if it were a numerical wind tunnel, and the author provided, for the case of the circular cylinder, a fine tuning of the main parameters that have an influence upon the calculated parameters. An optimization envelope was determined in terms of the domain of calculation length and width (to minimize blockage effects), best position for the centre of the cylinder, parameters that define the virtual wall representation as well as its spreading range, filters utilization, grid resolution, and the necessity, or not, of applying a white noise to trigger the shedding process. To exemplify, the introduction of noise was of necessity in three-dimensional simulations performed in 64 bits machines like the CRAY T94. Otherwise, a large extra computational time is required to trigger the vortex shedding mechanism when compared to a 32 bits machine, or when compared with the same 64 bits equipment with the resource of the white noise. Another important result was the finding that for typical two-dimensional cases the best value for L_y is $12d$ (d stands for the cylinder diameter); in spite of a difference of 4% in the value of the longitudinal velocity component at the lateral wall, the norm L^2 of the same component along the perimeter of the cylinder was on the same order as for $L_y = 32d$ and the influence on the Strouhal number was minimal.

3. RESULTS AND DISCUSSION

3.1 Preamble

In the introduction we have referred to a discontinuity at $Re = 64$ that appears at the laminar region of the Strouhal versus Reynolds number curve for the case of the circular cylinder (the limit of the laminar range is about $Re = 170$). This problem was experimentally investigated and duly clarified by Williamson (1989). The main point here is related to "end effects" at the tunnel walls. Independently of the spanwise length of the body, the influence of the kind of fixation at the walls will be, sooner or later, felt at the central station. Typically, an adequate way to isolate the tunnel wall boundary layer from the body wake is to use the so called end plates. These are thin stream-lined plates located close to the wall. By manipulating the end boundary conditions (basically the direction of the plates) Williamson was able to reproduce the different shedding régimes that appear in this situation. Positioning the plates in a way that they get aligned with the approaching flow and for $Re < 64$ oblique shedding is obtained with three spanwise cells with different stream-wise wave numbers. With the end plates in the same position but now running the tunnel at $Re > 64$ the central cell disappears, and the pattern is that of a chevron type with a large cell in the center that fits the end conditions by means of end oblique cells of different wave lengths. If the end plates are angled accordingly one can obtain a completely parallel shedding mode. Because the oblique shedding frequency can be collapsed upon the parallel curve taking into account the angle of obliquity, Williamson (1989) showed that, in practice, one can obtain an unique and continuous Strouhal curve.

With the growing of the Reynolds number the three-dimensional shedding keeps being laminar and parallel until about $Re = 170 - 190$, when mode A of shedding firstly appears. Further on, for Re on the order of 260 there gets installed the mode B shedding. In reality there is not a well defined frontier between the modes appearance. What happens in practice is a modes swapping up to the point when mostly mode B is found. The differences that characterize each pattern are related to the spanwise wave number — basically, $4d$ for mode A and $1d$ for mode B, in the case of the circular cross-sectional cylinder —, and the types of seeds of instability. The sequence of modes A and B, each one representing a discontinuity of the St x Re curve, constitutes a transition from laminar to turbulent status at the wake region. The next important event, say, will get installed at about $Re = 2000$, when the transition moves up to the primary shear layers and undulations will show up at the layers soon after they leave the body surface (see, for example, Persillon and Braza, 1998, Williamson, 1996, Henderson, 1997, Sumer and Fredsœ, 1997). In this section we will focus upon the topology of the flow about the circular cylinder and the body of Bearman, including some analysis of the modes of instability.

3.2 The Circular Cylinder

At the start of the study we have worked with the cylinder due to the wealth of literature data relative to this geometry. Figures 2, 3 and 4 show the three-dimensional vorticity fields for the following values of the Reynolds numbers: 150, 200, and 300. The Reynolds number 150 is still inside the laminar range, while the other values were chosen in the ranges of shedding modes A and B. Figures 5 and 6 illustrates further the topology of the streamwise structures that have appeared due to instabilities in the primary structures (the ones initially parallel to the cylinder axis). The reader can observe and confer that the spanwise wave number of the streamwise loops is basically $4d$ and $1d$ corresponding, respectively, to
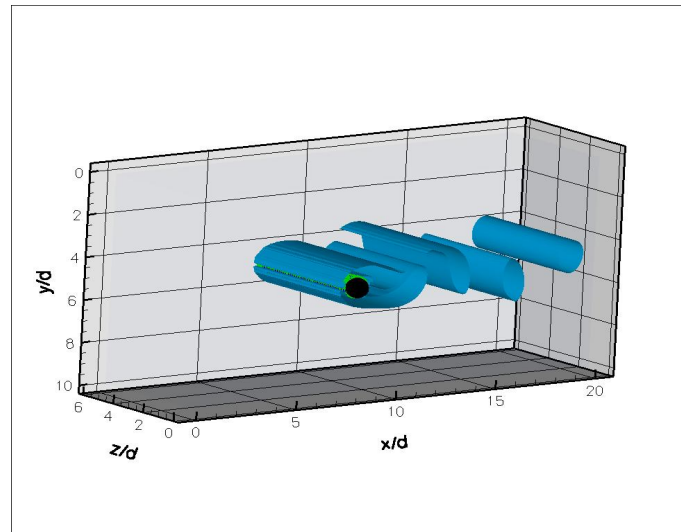
Figure 2. Three-dimensional view of flow about a circular cylinder. Vorticity iso-surfaces, $\omega = 0.43$. $Re = 150$.
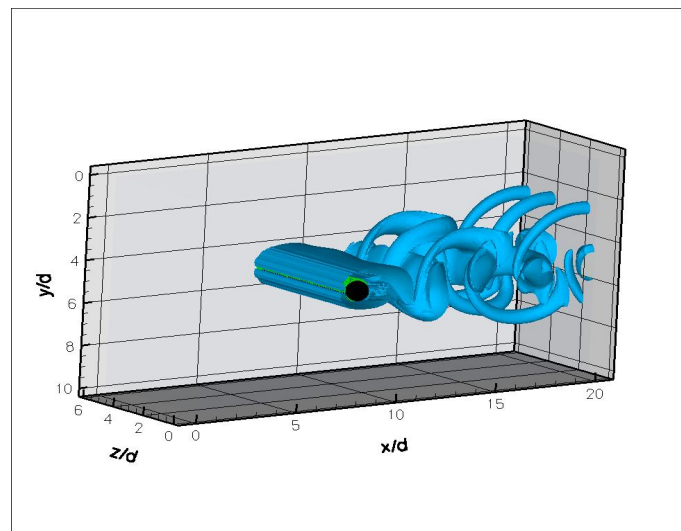
Figure 3. Three-dimensional view of flow about a circular cylinder. Vorticity iso-surfaces, $\omega = 0.43$. $Re = 200$.

modes A and B.

The grid that was employed in those runnings have the basic dimensions, $L_x = 20d$, $L_y = 10d$, and $L_z = 6d$. The grid is Cartesian and the cells are uniform; in those investigations, and independently of the Reynolds number, we have used 16 points per diameter in all three directions. The comparison with experimental data of Williamson (1992) as well as with other numerical simulations (Persilon and Braza, 1998, Mittal and Balachandar, 1995a) is very good. Another aspect that deserves to be noted is the outstanding qualities of code Incompact3d. Even with a grid that can be considered rather coarse, all the most important features of the flows in consideration are pretty well reproduced. Besides, the numerical dissipation is extremely low, so much so that we did not use any sort of "shedding inducer". The runnings were performed in a 64-bits machine, and the triggering device is basically the truncation error of the algorithm.

The reader is also invited to appreciate figure 7. These images represent cuts by planes yz of the field of flow. Frame (a) corresponds to a cut at $x_c/d = 2.0$ for the case of $Re = 200$, where x_c stands for the distance from the plane to the axis of the cylinder. In frame (b) the case is for $Re = 300$ and the distance from the plane yz to the axis is $3.0d$. We have kept the scales along the axis and the reader can promptly observe the correctness of the stream-wise wave number numerical predictions.

Another very important result is depicted on Fig. 8. Here we compare for the same Reynolds number, $Re = 300$, snapshots obtained from two- and three-dimensional simulations. In the 3-d case, Fig. 8(b) is obtained by cutting the instantaneous velocity field by an xy plane passing by the central spanwise station. The two frames correspond to approximately the same phase in the shedding cycle. There is an aspect that deserves careful attention. Let us compare the positions of the two large structures that are starting to leave the formation region. One can see that, in the three-dimensional case, the center of the primary vortex is situated in a position further downstream when compared to the
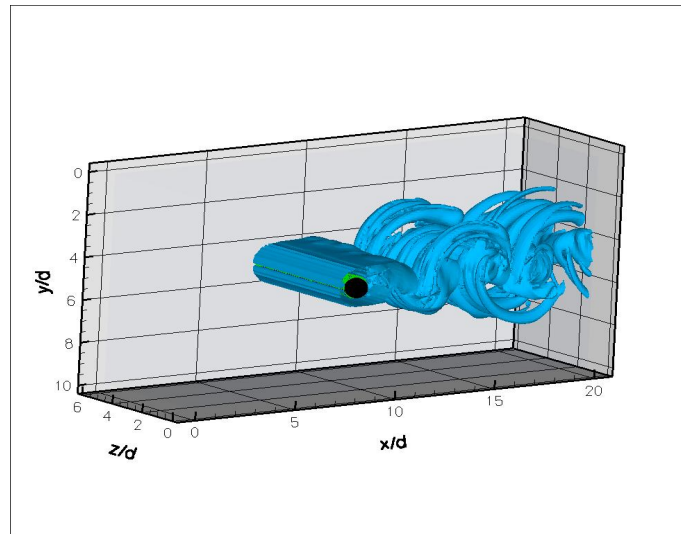
Figure 4. Three-dimensional view of flow about a circular cylinder. Vorticity iso-surfaces, $\omega = 0.43$. $Re = 300$.
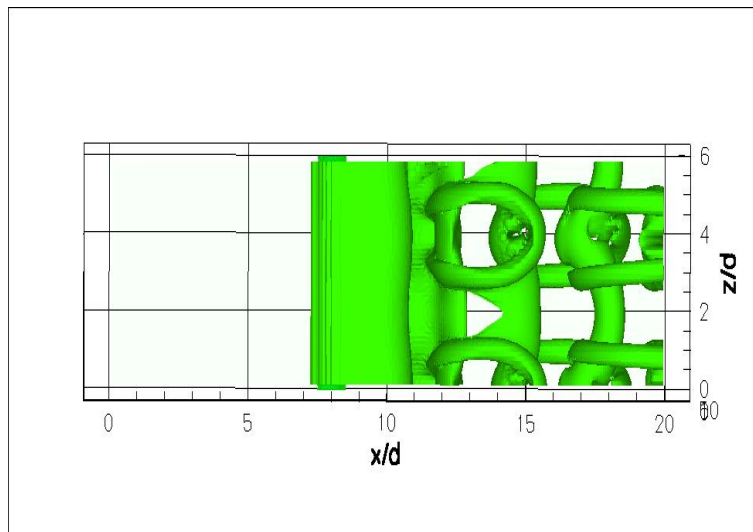
Figure 5. Top view of three-dimensional flow about a circular cylinder. Vorticity iso-surfaces, $\omega = 0.43$. $Re = 200$.
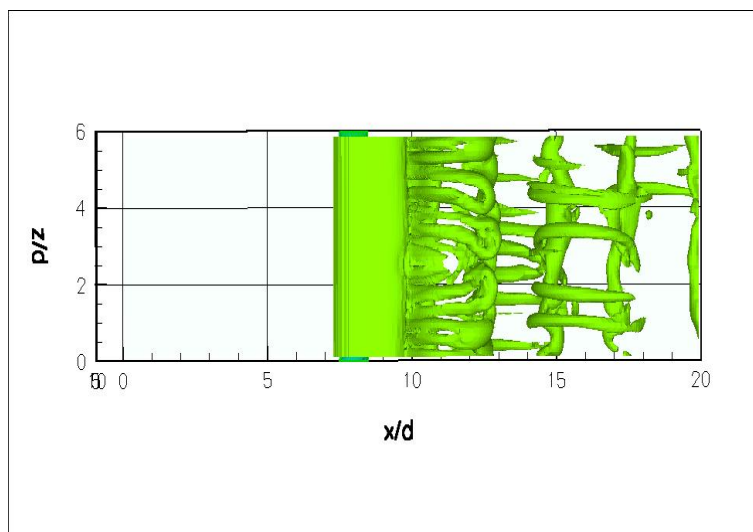
Figure 6. Top view of three-dimensional flow about a circular cylinder. Vorticity iso-surfaces, $\omega = 0.43$. $Re = 300$
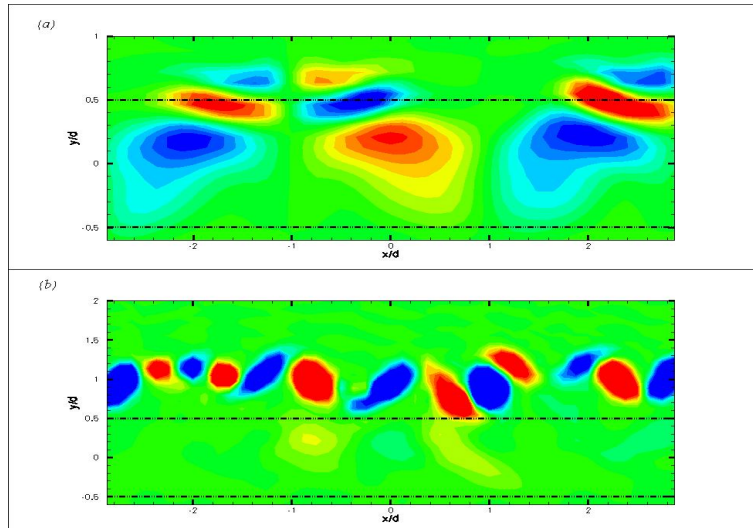
Figure 7. Cut view of three-dimensional flow about a circular cylinder. The dotted lines represent the view of the upper and lower surfaces of the cylinder by an observer looking upstream from the cut plane. Vorticity at planes yz: (a) $Re = 200$, $x_c/d = 2.0$, $-1.0 \leq \omega_x \leq 1.0$, 15 levels; (b) $Re = 300$, $x_c/d = 3.0$, $-1.0 \leq \omega_x \leq 1.0$, 15 levels.
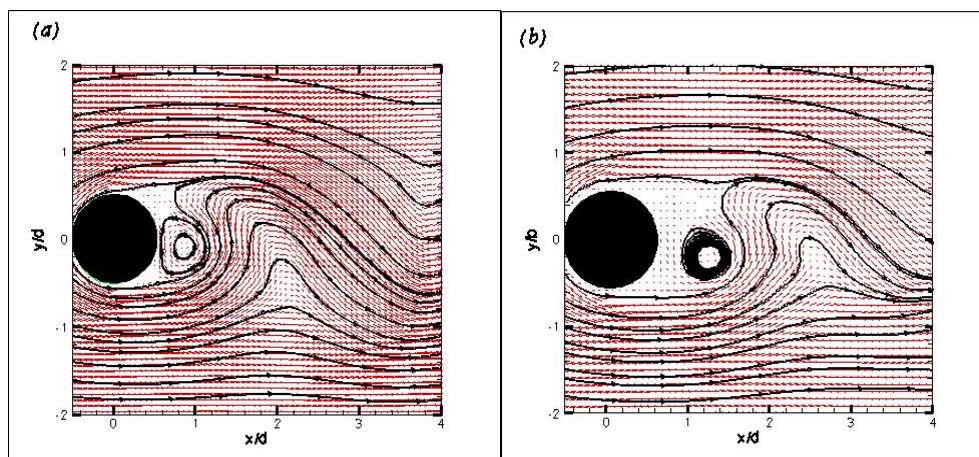
Figure 8. Comparison of the instantaneous velocity fields for the circular cylinder case. (a) Two-dimensional simulation; (b) Three-dimensional simulation: cut by a xy plane at the station $z = L_z/2$.
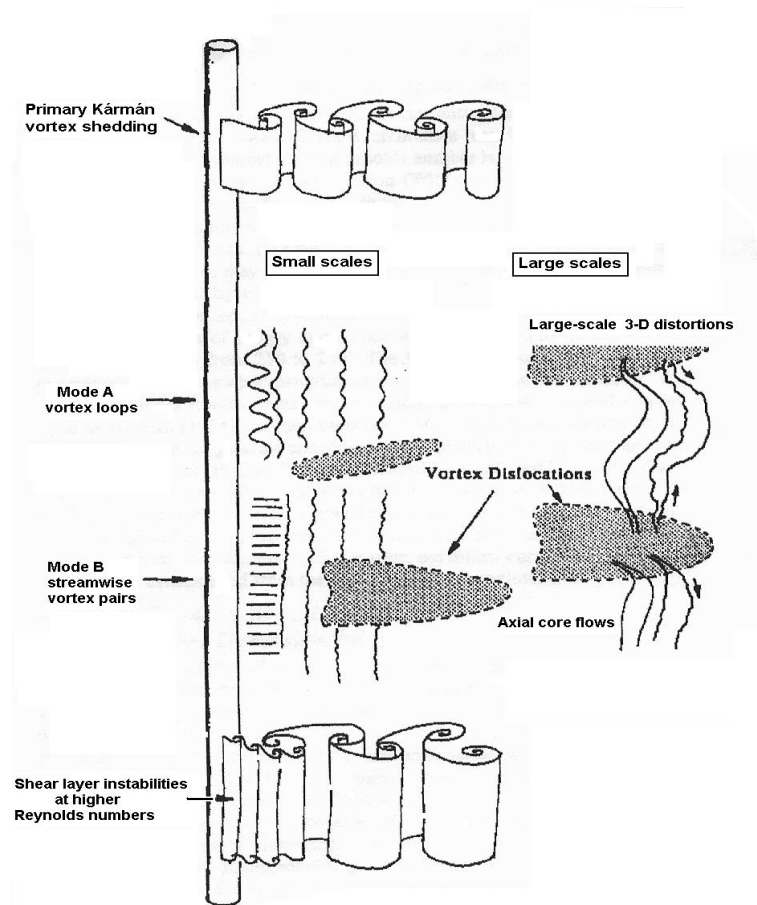
Figure 9. Schematic of the instabilities involved in the transition to turbulence (adapted from figure 5 of Williamson, 1996).

two-dimensional flow. The result of this is that, in the mean, the three-dimensional base pressure is larger when compared to the two-dimensional situation. The result is the fact that in general the global mean drag is lower in three-dimensional situations when confronted to two-dimensional ones, for the same Reynolds number (see Mittal and Balachandar, 1995a, for further details and comments).

The matter of the seeds of instabilities corresponding to modes A and B is also an important issue. By "seed of instability" we mean the first of all the perturbations. Mode A is explained by the effect of distortions of the primary structures as soon as they are shed. Distortions come from any kind of asymmetry inducing factor. After the first distortion, and if conditions are such that the instability is settled, then the system interfeeds itself, as we will later explain. In the case of wind tunnels, most of the time these asymetries are related to the level of turbulence coming embedded in the upstream flow. For numerical simulations the primary disturbing factor is the asymmetric distribution of the truncation error of the algorithm (that is why it is so important to have a low level of numerical dissipation in the code). Due to the Biot-Savart law there appears a stretching action and stream-wise loops are formed at the braids of the primary structures — see figures 5 and 9. The spanwise wave number of the loops in mode A is about $3 - 4$ diameters.

Most elusive to be understood is the mechanism that induces the mode B instability. Some authors argue (Williamson, 1996, Braza et al. 1990) that the instabilitiy seeding in this case comes from eventual oscillations of the primary shear layers, soon after they leave the surface of the body (Fig. 9). We have tried to check this argument by, first, simulating the two-dimensional flow for $Re = 2000$, which is about the condition for the appearance of the first oscillations at the shear layer — the transition would have come upstream to the position of the free layers. The reason for the simulation in two dimensions is to learn about the topology of the flow at those conditions. After that we simulated the three-dimensional situation for $Re = 300$ looking for any evidence of secondary instabilities at the shear layers.

The reader can observe in Fig. 10 the rolling of the shear layer coming from below. This is clear because the large main structure is already mostly formed in the close neighborhood. As both structures move downstream there will be a mutual interference, with frequency beatings and eventually vortex pairings (Braza et al., 1990). In figure 11 we show the field of flow in the rear of the cylinder for the case of the three-dimensional geometry. There is not any clear indication of any undulation of the free-shear layers. The Reynolds number is equal to 300 and at this level the mode B instability is already well installed — see Fig. 6. Anyhow, one can speculate in terms of a strong vorticity region formed below
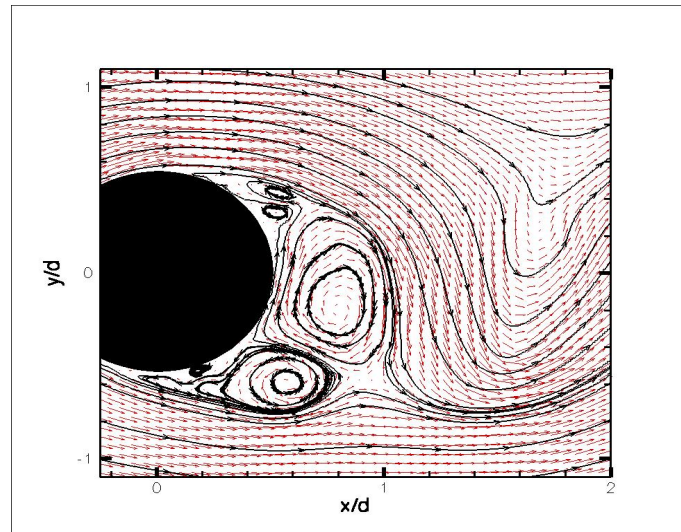
Figure 10. Two-dimensional instantaneous velocity field in the formation region of a circular cylinder. $Re = 2000$. The snapshot corresponds to a dimensionless time of 71.62.
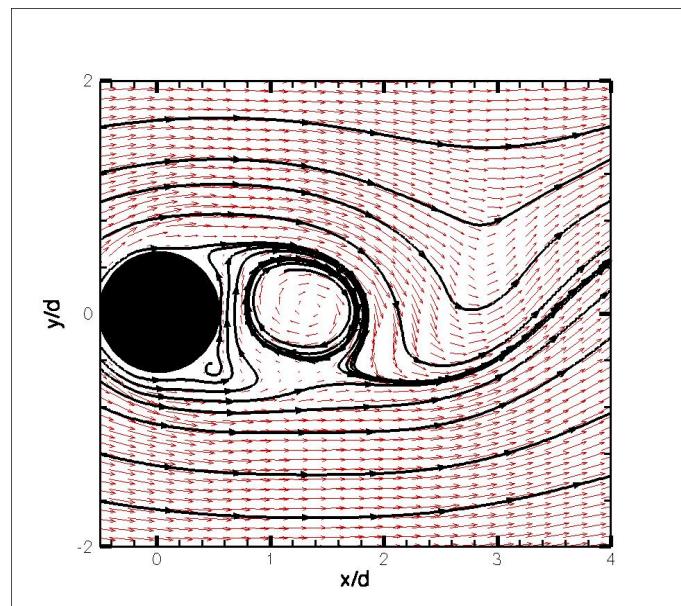
Figure 11. Instantaneous velocity field in the formation region of a circular cylinder. $Re = 300$. The figure corresponds to a cut of the three-dimensional flow domain by an xy plane passing by the spanwise central section of the cylinder. The snapshot corresponds to a dimensionless time of 339.3.
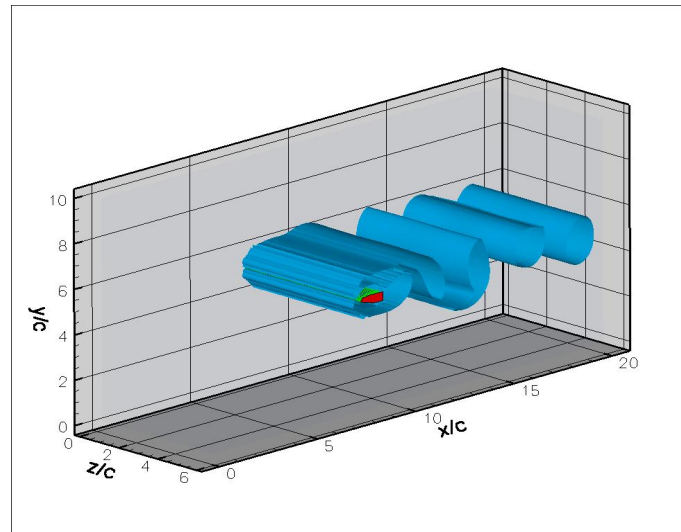
Figure 12. Instantaneous three-dimensional view of flow about the body of Bearman with $AR = 2.5$. $Re^h = 80$. Vorticity iso-surfaces, $\omega = 0.30$. $t = 148.79$
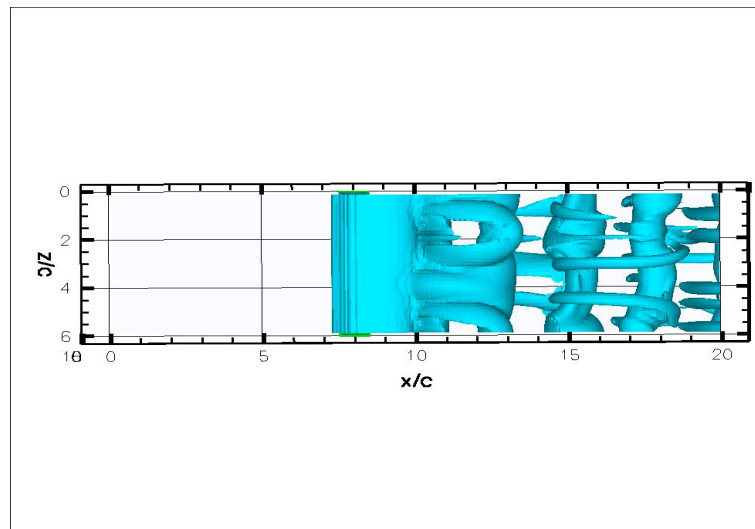
Figure 13. Top view of three-dimensional flow about the body of Bearman with $AR = 2.5$. $Re^h = 90$. Vorticity iso-surfaces, $\omega = 0.25$

the large structure. But, most probably, this straining region is a result of the blocking effect of the saddle point just in front. The part of the stream entering the region between the southwest converging separatrix and the northwest diverging separatrix is strongly deviated to the upper part of the wake between the large structure and the body. Braza et al. (1990) argue that in spite of no fluctuation evidences in the dettaching shear layers there are small periodic spots of vorticity at the lateral borders of the wake. These would be the downstream results of seeds of instability coming from the free shear layers. We have not, as yet, observed those effects. Most probably a much finer grid is needed because this is certainly a secondary effect.

3.3 The Body of Bearman

Recently, the present authors have performed a thorough analysis of the two-dimensional flow about a geometry we have called the body of Bearman (see the definition at the Introduction) (Ortega, Girardi and Silvestrini, 2009). There is an outstanding advantage in using this geometry for bluff bodies research because the boundary-layer separation points are fixed at the two corners at the base. Now our attention is devoted to the three-dimensional body with the incorporation of a certain spanwise length. The domain of calculation that was used at this very beginning part of the work is the same as for the circular cylinder, that is, $L_x = 20c$, $L_y = 10c$, and $L_z = 6c$, where c is the chord of the body (the distance between the leading edge of the body and the central point of the vertical base). The spanwise length of the body is $6c$. As for the case of the cylinder, and also for comparison purposes, we have used the same number of points per chord, i.e.,
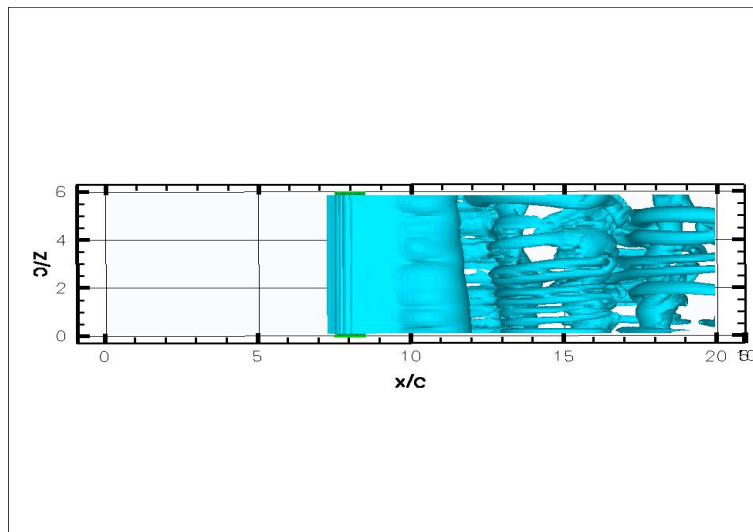
Figure 14. Top view of three-dimensional flow about the body of Bearman with $AR = 2.5$. $Re^h = 120$. Vorticity iso-surfaces, $\omega = 0.45$.

16, independently of the Reynolds number.

Ryan, Thompson and Hourigan (2005) have performed a Floquet stability analysis of this form for several values of the aspect ratio, AR, which is defined as the ratio of chord and base height of the body. They have discovered other modes of instability besides modes A and B for the circular cylinder. Anyway mode A is very similar in topology to the circular cylinder case, but with some differences in dimensions. As the authors have found mode A is the most unstable of all modes for the case of short cylinders. Anyhow, it is not clear from their results what is the value of the Reynolds number for which mode A appears for the first time. For $AR = 2.5$ and $\lambda/h = 7$ they argue that the instability mode first becomes unstable at a Reynolds number approximately equal to 240. (λ is the spanwise wave number). For $Re^h = 250$ (the superscript h indicates that the reference length for the definition of the Reynolds number in this case is the body base height) the unstable mode range is $3.5 < \lambda/h < 10$, what characterizes a broad band instability. With the growing of the Reynolds number the wavelength diminishes and for $Re^h = 400$ the wave length is about $3.5h$. We shall try to find by means of straight simulations — without resorting to a Floquet analysis strategy, but using only code Incompact3d —, for what value of the Reynolds number the mode A instability appears for the first time in the case $AR = 2.5$.

A certain range of Reynolds numbers was investigated, basically between 60 and 400. The Reynolds number (based on h) for the onset of three-dimensionalization is greater than 80 and smaller than 90. Figures 12 and 13 are testimony of this fact. We are at present trying to narrow this gap, and besides we shall try to discover how is the scenario as the Reynolds number grows. In the case of the circular cylinder we already know that there is another instability when mode B starts to dominate the topology of the near wake. It is important to discover if there is also a sharp frontier of this type for the case of the body of Bearman. One should keep in mind that three-dimensional simulations are very costy, takes lots of CPU time, and, to make matters worse, the investigation at a transition region normally asks for long runnings of the code, where the minimum time of calculation may reach a thousand units, or even more (Ortega, Girardi and Silvestrini, 2009).

On the other hand, the data already obtained is able to support many important observations and conclusions. For example, the streamwise wave number for $Re^h = 120$ is not well defined — see the snapshot in Fig. 14. There are formations with $\lambda = 1c$ typical of mode B for the cylinder and $\lambda = 3c$, typical of mode A. One should also note that the structures located farther from the body, and that comes from a former shedding cycle, are larger and with, in general, larger wave numbers when compared to the ones that are closer to the body. Most probably what is happenning here is the same phenomenon of modes swapping, also typical of the circular cylinder geometry.

Also very illustrative are the frames in Fig. 16. One can observe the evolution of the structures that will configure the topology of mode A type of instability for the body of Bearman. As time passes the distortion of the basic Kármán rollers induce the formation of streamwise "arms" that will elongate and reach the braids of the next basic structure. This elongation is a result of the streamwise arms stretching by the action of the basic rollers, and this is a very important factor in the final three-dimensionality of the near wake. The rollers by themselves suffer the stretching action of the streamwise formations, and this is absolutely evident from Fig. 15. Each streamwise loop has arms which are counter-rotating, therefore, their effect is to contract "inside" and stretch "outside". This teaches us that the interaction of basic rollers and streamwise loops are instrumental for the definition of the topology at the wake cavity.

Another very important point is related to the origin of the streamwise arms. Experimental flow visualizations (Nygaard and Glezer, 1991, Williamson, 1992) show some dye escaping from the main formation and into the braid regions.
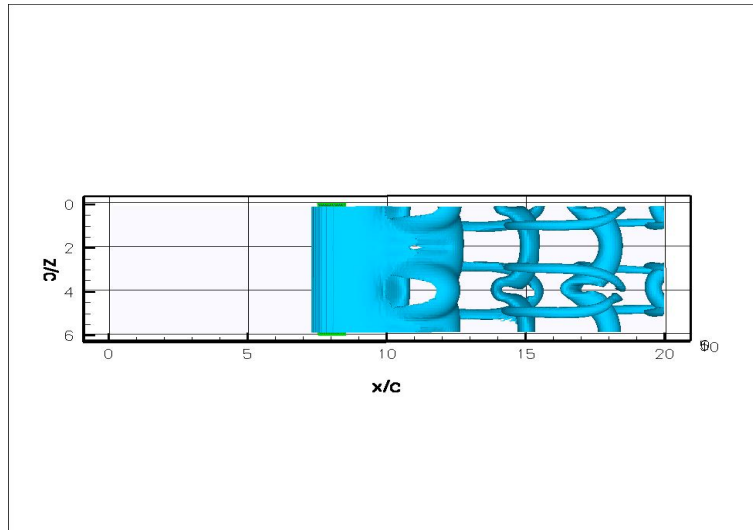
Figure 15. Top view of three-dimensional flow about the body of Bearman with $AR = 2.5$. $Re^h = 160$. Vorticity iso-surfaces, $\omega = 0.70$.
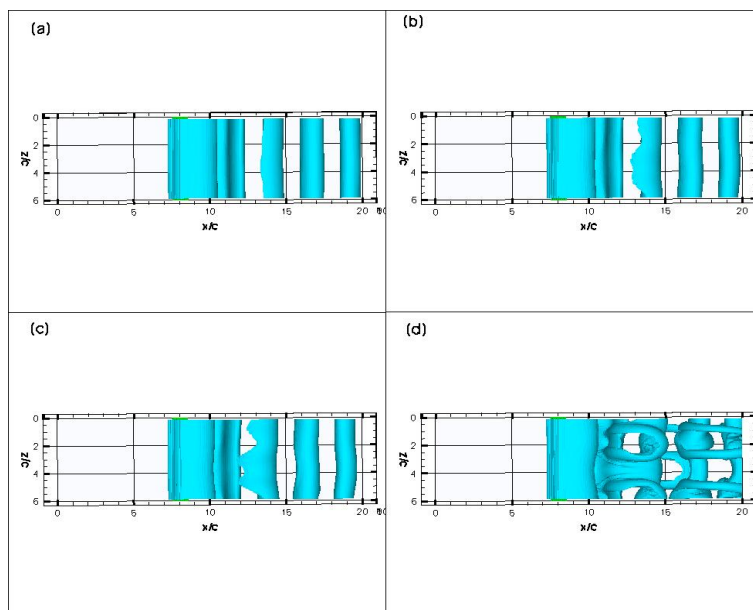
Figure 16. Top views of three-dimensional flow about the body of Bearman with $AR = 2.5$ (flow from left to right). $Re^h = 90$. Vorticity iso-surfaces, $\omega = 0.3$. (a) $t = 127.42$; (b) $t = 143.65$; (c) $t = 148.79$; (d) $t = 171.57$.

These are then stretched and gives rise to the streamwise arms we have referred above. On the other hand, numerical investigations by Mittal and Balachandar (1995a, 1995b) seem to indicate that due to the hard stretching of the basic roll in localized spanwise stations (see Fig. 15) some *"pieces of the deformed core break off and enter the neck region, where they get stretched to form streamwise structures"*. The very starting of the arms formation, which is configured on Fig. 16(a) and (b), seems to corroborate the former point of view.

4. Conclusions

The first results of a research work that deals with three-dimensional flows about two-dimensional type geometries are presented and discussed. The first cases corresponded to the circular cylinder with the basic aim of comparing data with the literature. In general the results are quite good and compares very well. In the sequel we have started to study the body of Bearman. The main goal here is to try to assess the behaviour of modes A and B for a range of low Reynolds numbers. As yet, we have concentrated upon a small value of the aspect ratio, $AR = 2.5$, what characterizes it as a short cylinder. The idea of a short cylinder at the beginning is to compare data with the circular cylinder. The study is not finished yet, but one can observe that, in principle, the overall scenario is rather similar to the circular cylinder with main differences localized upon dimensions and not upon basic concepts. On the other hand, it is very important to investigate also at the upper range of Reynolds numbers where, much probably, other differences will show up.

5. REFERENCES

Barkley, D. and Henderson, R.D., 1996, "Three-dimensional Floquet Stability Analysis of the Wake of a Circular Cylinder", Journal of Fluid Mechanics, 322, pp. 215-241.

Bearman, P.W., 1965, "Investigation of the Flow Behind a Two-Dimensional Model with a Blunt-trailing Edge and Fitted with Splitter Plates. Journal of Fluid Mechanics, 21, part 2, pp. 241-255.

Braza, M., Chassaing, P., and Ha Minh, H., 1990, "Prediction of Large-Scale Transition in the Wake of a Circular Cylinder", Physics of Fluids A, pp. 1461-1471.

Fadlun, E.A., Verzicco R., Orlandi, P. and Mohd-Yusof, J., 2000, " Combined immersed-boundary finite-difference methods for three-dimensional complex flow simulations". Journal of Computational Physics, 161, pp. 35-60.

Goldstein, G., Handler, R., and Sirovich, L., 1993 "Modeling a no-slip flow boundary with an external force field". Journal of Computational Physics, 105, pp. 354-366.

Henderson, R.D., 1997, "Nonlinear Dynamics and Pattern Formation in Turbulent Wake Transition", Journal of Fluid Mechanics, 352, pp. 65-112.

Lamballais, E., 1996, "Numerical Simulation of the Turbulence in a Plane Rotating Channel". Ph.D. Dissertation, National Polytechnic Institute of Grenoble. (in french)

Lamballais, E., and Silvestrini, J.H., 2002 "Direct numerical simulation of interactions between a mixing layer and a wake around a cylinder", Journal of Turbulence, 3, 028.

Lardeau, S., Lamballais, E., and Bonnet, J.P., 2002, "Direct Numerical Simulation of a Jet Controlled by Fluid Injection", Journal of Turbulence, 3, p. 002.

Lele, S., 1992, "Compact finite difference schemes with spectral-like resolution". Journal of Computational Physsics, 103, pp. 16-42.

Mittal, R., and Balachandar, S., 1995a, "Effect of Three-Dimensionality on the Lift and Drag of Nominally Two-Dimensional Cylinders", Physics of Fluids, 7 (8), p. 1841.

Mittal, R., and Balachandar, S., 1995b, "Generation of Streamwise Vortical Structures in Bluff Body Wakes", Physical Review Letters, 75, 7, p. 1300.

Nygaard, K.J., and Glezer, A., 1991, "Evolution of stream wise vortices and generation of small-scale motion in a plane mixing layer", Journal of Fluid Mechanics, 231, p. 257.

Ortega, M.A., and Silvestrini, J.H., 2004, "A DNS prediction of the flow around an airfoil at high angles of attack", AIAA Paper 2004-5079.

Ortega, M.A., Girardi, R.M., and Silvestrini, J.H., 2007, "The formation region behind a blunt body fitted with a splitter plate", AIAA Paper 2007-1306.

Ortega, M.A., Girardi, R.M., and Silvestrini, J.H., 2009, "On the Wake Behind a Blunt-Trailing-Edged Body: A Basic Study", CFD Report 09, Department of Aerodynamics, ITA, São José dos Campos, SP, Brazil.

Persillon, H., and Braza, M., 1998, "Physical Analysis of the Transition to Turbulence in the Wake of a Circular Cylinder by Three-Dimensional Navier-Stokes Simulation", Journal of Fluid Mechanics, 365, pp. 23-88.

Ribeiro, P.A.R., 2002, "The control of the vortexes shedding mechanism in the wake of circular cylinders by means of numerical simulation", M.Sc. Thesis, Federal University of Rio Grande do Sul, Porto Alegre, RS, Brazil. (in portuguese)

Roshko, A., 1954, "On the Development of Turbulent Wakes from Vortex Streets", NACA Report 1191.

Silvestrini, J.H., and Lamballais, E., 2004, "Direct numerical simulation of oblique vortex shedding from a cylinder in shear flow", International Journal of Heat and Fluid Flow, 25, 3, pp. 461-470.

Sumer, B.M., and Fredsœ 1997 "Hydrodynamics Around Cylindrical Structures", World Scientific, London, UK.

Thompson, M.C., Leweke, T., and Williamson, C.H.K., 2001, "The Physical Mechanism of Transition in Bluff Body Wakes", Journal of Fluids and Structures, 15, pp. 607-616.

Tritton, D.M., 1959, "Experiments on the Flow Past a Circular Cylinder at Low Reynolds Numbers", Journal of Fluid Mechanics, 6, p. 547.

Williamson, C.H.K., 1988, "The Existence of Two Stages in the Transition to Three-Dimensionality of a Cylinder Wake", Physics of Fluids, 31, p. 3165.

Williamson, C.H.K., 1989, "Oblique and Parallel Modes of Vortex Shedding in the Wake of a Circular Cylinder at Low Reynolds Number", Journal of Fluid Mechanics, 206, pp. 579-627.

Williamson, C.H.K., 1991, "Turbulent Shear Flows 7", Springer Verlag, Berlin, p. 173.

Williamson, C.H.K., 1996, "Vortex Dynamics in the Cylinder Wake", Annual Review of Fluid Mechanics, 28, pp. 477-539.

6. Responsibility notice

The author(s) is (are) the only responsible for the printed material included in this paper